

γ -Al₂O₃ Viewed as a Defect Oxyhydroxide

γ -Al₂O₃ is commonly used as a catalyst support (1-3). Among the investigators who have studied the alumina system, Lip-pens has compiled an excellent overview of the aluminum hydroxide-aluminum oxide phases (4). Peri has modeled the dehydroxylation of a (100) surface plane of γ -Al₂O₃ via a Monte Carlo calculation (5). By assuming that during dehydroxylation neither two O²⁻ ions nor two Lewis sites occupy adjacent positions, Peri calculated a maximum surface dehydroxylation of 67%. Relaxing these assumptions increased the percentage of removable surface hydroxyls to 90%. Complete dehydroxylation, Peri concluded, requires mobile surface ions. This conclusion agrees with the observation that conversion of γ -Al₂O₃ to α -Al₂O₃ requires a minimum critical temperature rather than a prolonged isothermal heating at a lower temperature. Butt has compared the Monte Carlo simulation with experimental results of ethanol dehydration (6).

In a separate study, Knozinger discussed the probable hydroxyl surface site geometries of γ -Al₂O₃ (7). He assumed that γ -Al₂O₃ adopts an ideal spinel structure and forms crystallites bounded by low index planes. Since five distinct aluminum nearest neighbor environments may occur for terminal OH groups, this model dramatically illustrates the heterogeneity of the γ -Al₂O₃ surface. In this discussion, we propose a modified formulation for a γ -Al₂O₃ precursor, and develop a number of discrete limitations on some of its physical properties.

Any description of γ -Al₂O₃ must include the known structural features, dehydroxylation behavior, physical properties (such as surface area and pore volume), and relationship to other aluminas. Powder X-ray diffraction has established that γ -Al₂O₃

crystallizes with a spinel-related structure (4). Unlike silica or silica-alumina support materials, γ -Al₂O₃ is not amorphous. X-Ray line broadening indicates that the average particle size measures 80-90 Å (8). Infrared studies have shown that γ -Al₂O₃ contains an hydroxylated surface (9, 10). During thermal treatment over the temperature range 200-1100°C, γ -Al₂O₃ loses water as neighboring hydroxyl groups condense. Complete dehydroxylation produces α -Al₂O₃. Typical surface areas and pore volumes of γ -Al₂O₃ range from 150 to 230 m²/g and from 0.4 to 0.8 cm³/g, respectively. Occasionally, reports quote surface areas of γ -Al₂O₃ as high as 300 m²/g. We will present arguments below which support the contention that these aluminas retain an amorphous component, and, in fact, are not pure γ -Al₂O₃.

A large number of metal and mixed metal oxides crystallize with a spinel structure (11-13). This structure consists of a cubic close-packed lattice of oxygens with one-eighth of the tetrahedral and one-half of the octahedral interstices filled by cations (see Fig. 1). The resulting arrangement contains strings of edge-shared octahedra linked via edge sharing to orthogonal strings in planes above and below, and via corner sharing to bridging tetrahedra.

In the general formulation of spinel as AB₂O₄, A and B represent cations and O represents oxygen. Note that the cation to anion ratio in spinel equals 3/4. Wells, in his treatise describes γ -Al₂O₃, as Al_{8/3}□_{1/3}O₄ (14), consistent with the constraints of stoichiometry and electrical neutrality. This formulation of an alumina spinel would accurately describe the case of large elementary particles containing only a small fraction of anions on the surface. However, in the case of γ -Al₂O₃ (in its fully hydroxyl-

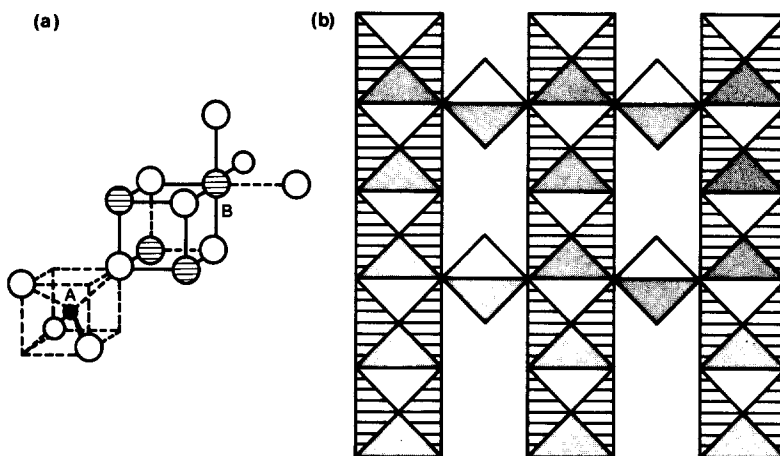


FIG. 1. Spinel. (a) Section showing tetrahedral (A) and octahedral (B) cations. (b) Projection on (100) showing edge-shared octahedra connected by corners to tetrahedra.

ated or precursor state) a significant fraction of the anions (in the form of OH groups) do occupy the surface of a particle. By including these OH groups, we arrive at a modified description of $\gamma\text{-Al}_2\text{O}_3$.

We present two approaches for including the OH groups; both lead to the same results. In both approaches, we allow the number of vacancies to deviate from 1 per every 9 cation sites. In the first case, replacement of $y/2$ O^{2-} ions by y $(\text{OH})^-$ ions maintains electrical neutrality: $\text{Al}_{8/3}\square_{1/3}\text{O}_4$ becomes $\text{Al}_{8/3}\square_x\text{O}_{4-y/2}(\text{OH})_y$. Solving for x and y requires two relationships. First, stoichiometry fixes the cation: anion ratio at $\frac{3}{4}$.

$$\begin{aligned} \text{No. cation sites/No. anion sites} \\ = \frac{8/3 + x}{4 + y/2} = 3/4, \end{aligned}$$

or

$$y = 8/3(x - \frac{1}{3}). \quad (1)$$

The weight loss during dehydroxylation of $\gamma\text{-Al}_2\text{O}_3$ and conversion to $\alpha\text{-Al}_2\text{O}_3$ provides a means for deriving a second equation relating x and y . Upon complete dehydroxylation, the following transformation occurs:

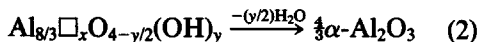


Figure 2 plots the weight loss as a function of x/y (i.e., the ratio of vacancies to OH groups) during complete dehydroxylation

for the series of hypothetical phases $\text{Al}_{8/3}\square_x\text{O}_{4-y/2}(\text{OH})_y$, $0.5 < x/y < 10$. That is, we choose a value of x , calculate y from Eq. (1), plot the abscissa as the ratio x/y , and calculate the weight loss percentage for this value of y from Eq. (2). The experimental values determined on a series of $\gamma\text{-Al}_2\text{O}_3$ samples by measuring the weight loss between 200 and 1200°C very closely bracket a ratio of 1 for x/y . This important result implies that the number of cation vacancies equals the number of hydroxyl groups. For x equal to y , Eq. (1) solves for $x = \frac{8}{15}$. Renormalizing the result (by multiplying the coefficients by $4/(4 + y/2)$) reestablishes the total anion count to four and yields a $\gamma\text{-Al}_2\text{O}_3$ precursor of stoichiometry $\text{Al}_{2.5}\square_{.5}\text{O}_{3.5}(\text{OH})_{.5}$.

In the second approach, the total anion

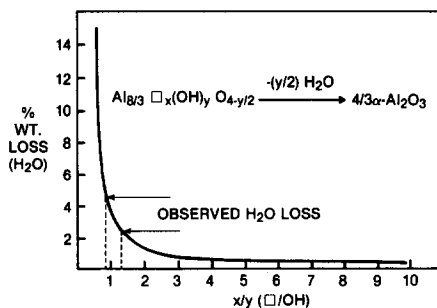


FIG. 2. Dehydroxylation of $\gamma\text{-Al}_2\text{O}_3$. The observed water loss brackets a value of x/y (\square/OH) of one.

count is fixed at 4 and the stoichiometric and electrical neutrality constraints are maintained by creating additional cation vacancies: $\text{Al}_{8/3}\square_{1/3}\text{O}_4$ becomes $\text{Al}_{(8/3)-x'}\square_{(1/3)+x'}\text{O}_{4-y'}(\text{OH})_{y'}$. Electrical neutrality requires that $y' = 3x'$. Combining this result with the percent water lost during dehydroxylation as a function of y yields values $y' = \frac{1}{2}$, $x' = \frac{1}{6}$. The $\gamma\text{-Al}_2\text{O}_3$ precursor again becomes $\text{Al}_{2.5}\square_{.5}\text{O}_{3.5}(\text{OH})_{.5}$. In this modified form of Wells' equation, the number of cation vacancies has changed to 1 in 6 from 1 in 9. Although we do not actually know if the vacancies occur on tetrahedral or octahedral sites, this formula implies that either $\frac{1}{2}$ of the normally occupied tetrahedral or $\frac{1}{4}$ of the octahedral sites in a spinel are vacant. The closest parallel to this formulation in the literature was discussed briefly at a conference thirty years ago (15). More traditional representations of $\gamma\text{-Al}_2\text{O}_3$ as the defect spinel $\text{Al}_{2.8/3}\square_{1/3}\text{O}_4$ (14), or as a hydrogen (non-defect) spinel HAl_5O_8 (16) ignore the nature of the surface hydroxyl groups. Although the formula presented here can be rewritten in a strictly formal sense as $\text{Al}_2\text{O}_3 \cdot 1/5\text{H}_2\text{O}$, this representation proves useful only for comparative purposes, since $\gamma\text{-Al}_2\text{O}_3$ is definitely not a crystalline hydrate.

The following table outlines the thermal genesis of the family of aluminas with both the formal representation and the actual stoichiometry of the phases.

Notice that the $\gamma\text{-Al}_2\text{O}_3$ precursor now "fits" logically into a family of aluminas

starting with the trihydroxide, and progressing to the stoichiometric oxyhydroxide, passing through the transitional or oxide-rich oxyhydroxides, and finally reaching the anhydrous pure oxide, $\alpha\text{-Al}_2\text{O}_3$.

Before exploring the significance of this new formulation of $\gamma\text{-Al}_2\text{O}_3$ note that two questions remain unresolved: (1) the physical significance of having an equal number of vacancies and hydroxyl groups, (2) the distribution of the vacancies on the tetrahedral and octahedral sites. Vacancies often diffuse toward surfaces so one can speculate that vacancies exist in an enhanced concentration there.

The consequences of formulating the $\gamma\text{-Al}_2\text{O}_3$ precursor as $\text{Al}_{2.5}\square_{.5}\text{O}_{3.5}(\text{OH})_{.5}$ are described below. If the hydroxide ions populate only the surface and the oxide ions comprise the bulk of $\gamma\text{-Al}_2\text{O}_3$ particles, the fraction of anions on the surface becomes 1 in 8:

fraction anions on surface

$$= \frac{(\text{OH})_{\text{surf}}}{(\text{OH})_{\text{surf}} + \text{O}_{\text{bulk}}} = \frac{0.5}{0.5 + 3.5} = 1/8. \quad (3)$$

Furthermore, if a hypothetical crystal shape is chosen, a number of fundamental physical properties follow. A logical choice places the most densely packed planes on the surface—the lowest energy configuration. Since $\gamma\text{-Al}_2\text{O}_3$ crystallizes in a slightly distorted cubic cell (tetragonal, $a = 7.96 \text{ \AA}$, $c = 7.81 \text{ \AA}$ (17)), with an approximate cubic

Formal representation	Stoichiometry	Common name
$\text{Al}_2\text{O}_3 \cdot \text{H}_2\text{O}$	$\text{Al}(\text{OH})_3$	Gibbsite Bayerite
$\text{Al}_2\text{O}_3 \cdot \text{H}_2\text{O}$	$\text{AlO}(\text{OH})$	Boehmite
$\text{Al}_2\text{O}_3 \cdot 1/5\text{H}_2\text{O}$	$\text{Al}_{2.5}\square_{.5}\text{O}_{3.5}(\text{OH})_{.5}$	$\gamma, \eta\text{-Al}_2\text{O}_3$
Al_2O_3	Al_2O_3	$\alpha\text{-Al}_2\text{O}_3$

increasing calcination
 temperature and
 degree of
 dehydroxylation
 ↓



FIG. 3. γ - Al_2O_3 particle. The spheres represent the closest packing of the anions. The eight triangular faces correspond to the set of (111) planes of a cube.

closest packing of the anions, a particle with the most densely packed planes on the surface will assume the shape of an octahedron—that is, a cube cut with its (111) faces exposed. Undoubtedly other low index planes such as (110) or (100) exist, but for simplicity (and because the calculations are not extremely sensitive to the planes chosen), octahedral particles are assumed for the following discussion. Subtle differences in the surface or catalytic properties of γ - or η - Al_2O_3 may result from generating different ratios of these surface planes by use of different precursors or conditions of preparation.

Figure 3 represents a particle of γ - Al_2O_3 ; the spheres depict the anions in a cubic closest packed arrangement. Simple volume versus particle size relationships can establish the size of the octahedra that has $\frac{1}{8}$ of its anions on the surface. An arithmetic progression relates the number of anions on the surface to the number of anions on an edge of the octahedron (N):

$$\begin{aligned} \text{No. anions on surface} \\ &= [N + 2(N - 1) + (N - 2)] + 2[(N - 1) \\ &\quad + 2(N - 2) + (N - 3)] + \cdots + 2 \\ &= 4(N - 1)^2 + 2. \end{aligned} \quad (4)$$

Similarly, a geometric series relates the total number of anions in the particle to the

number of anions on an edge of the octahedron:

$$\begin{aligned} \text{No. total anions} &= N^2 + 2[(N - 1)^2 \\ &\quad + (N - 2)^2 + (N - 3)^2 + \cdots] \\ &= \frac{N(2N^2 + 1)}{3}. \end{aligned} \quad (5)$$

The ratio of surface anions to total anions then becomes:

$$\frac{4(N - 1)^2 + 2}{N(2N^2 + 1)/3} \quad (6)$$

which for large values of N reduces to

$$\frac{4N^2}{(2/3)N^3} \approx \frac{6}{N}. \quad (7)$$

Equating expression (6), the ratio of surface anions to total anions, to $\frac{1}{8}$, yields a value of 46 for N . Thus, 46 anions would populate each edge of an octahedrally shaped γ - Al_2O_3 particle. With an oxygen covalent radius of 1.24 Å (18), the edge of the idealized γ - Al_2O_3 particle becomes 115 Å, in reasonable agreement with X-ray line broadening measurements which suggest a value of 80–90 Å.

Crystallite size and density limit the specific surface area (m^2/g) of the octahedral particle. The following relationship defines the actual surface area of the octahedral particle in questions (e = edge length of the octahedron):

$$\begin{aligned} \text{surface area} &= 8 \times \left(\frac{1}{2}\right) \left(e \frac{\sqrt{3}}{2}\right) \times e \\ &= 2\sqrt{3} e^2 = 4.5 \times 10^4 \text{ \AA}^2. \end{aligned} \quad (8)$$

Similarly, the following formula defines the volume of the octahedron:

$$\begin{aligned} \text{volume} &= 2 \times \frac{1}{3} e^2 \left(\frac{3}{\sqrt{2}}\right) e \\ &= \frac{\sqrt{2}}{3} e^3 = 7.0 \times 10^5 \text{ \AA}^3. \end{aligned} \quad (9)$$

Reported values of the density of γ - Al_2O_3 vary around $\sim 3.5 \text{ g/cm}^3$. A computed value based on the reported cell constants of $a = 7.96$, $c = 7.81 \text{ \AA}$ (for a tetragonal cell) (17) yields a density of 3.78 g/cm^3 :

$$\rho_{\text{calc}} = \frac{140.75 \text{ g/mol} \times \frac{1 \text{ mol}}{6.023 \times 10^{23} \text{ molecules}} \times \frac{8 \text{ molecules}}{\text{unit cell}}}{(7.96 \text{ \AA})^2(7.81 \text{ \AA}) \times \left(\frac{10^{-8} \text{ cm}}{\text{Å}}\right)^3} = 3.78 \text{ g/cm}^3. \quad (10)$$

With a value of 3.5–3.8 g/cm³ for the density, the calculated specific surface area lies somewhat below 200 m²/g:

$$\sigma = \frac{\text{surface area}}{\text{volume} \times \text{density}} = 170\text{--}185 \text{ m}^2/\text{g} \quad (11)$$

This range agrees well with reported surface areas.

In a simplified approach, consider the micropore volume of the material as simply the void space created within the packing of the individual octahedral particles. The most-dense and least-dense packing configuration of $\gamma\text{-Al}_2\text{O}_3$ octahedra should bracket the limiting values of pore volume. Assuming the octahedra touch minimally at their tips, the least densely packed configuration consists of a three-dimensional array of corner-shared octahedra. Figure 4 illustrates this array with a cube of edge ϵ enclosing this array. Since the total volume of the enclosed cube (V_c) is ϵ^3 , the volume enclosed by the 8 $\gamma\text{-Al}_2\text{O}_3$ particles that each have $\frac{1}{8}$ of their volumes in the cube equals

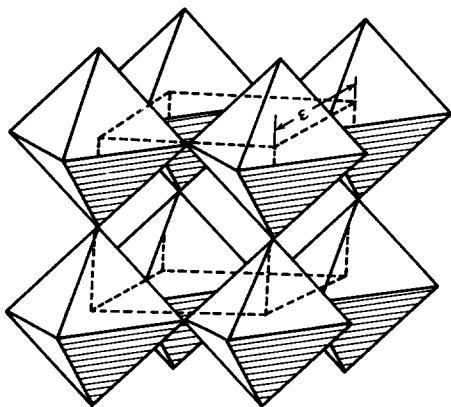


FIG. 4. Least-dense packing of $\gamma\text{-Al}_2\text{O}_3$. Pore volume = 1.3 cm³/g.

$$8 \times \frac{1}{8} \times \text{vol}_{\text{oct}} = \frac{\sqrt{2}}{3} \left(\frac{\epsilon}{\sqrt{2}}\right)^3 = \epsilon^3/6. \quad (12)$$

Thus the volume occupied by the $\gamma\text{-Al}_2\text{O}_3$ particles is $V_c/6$, the volume of the void space is $5V_c/6$, so that the pore volume becomes 1.3 cm³/g:

$$\begin{aligned} \text{pore volume} &= \frac{\text{vol void space}}{\text{wt alumina}} \\ &= \frac{5V_c/6}{(V_c/6)\text{density}} \approx 1.3 \text{ cm}^3/\text{g}. \quad (13) \end{aligned}$$

The low pore volume case follows a similar argument yielding 0.04 cm³/g as a limit. Hence, the theoretical micropore volume of $\gamma\text{-Al}_2\text{O}_3$ lies between 1.3 and 0.04 cm³/g, respectively.

It is important to note again that in this treatment of $\gamma\text{-Al}_2\text{O}_3$, an equilibrium fully hydroxylated (precursor) state of the material is considered. However, the transitional aluminas dynamically change as they are subjected to thermal treatment. $\gamma\text{-Al}_2\text{O}_3$, for example, will lose hydroxyl groups when heated above 200°C. At temperatures near $\sim 800^\circ\text{C}$, the surface area decreases, the particle size and bulk density increases. This can be rationalized by a mechanism in which two adjacent particles coalesce and a terminal oxide ion (formed when two OH groups condense to form water) become incorporated as a bulk anion bridging the two particles. In this manner, the particle grows and the effective surface area decreases. This mechanism also provides for a gradual annihilation of vacancies. The transitional aluminas pass through a range of surface areas down to $\sim 30 \text{ m}^2/\text{g}$. It is interesting that minor structural alterations also take place, such as a change in symmetry (to monoclinic) and an appearance of a crystallographically distinct phase ($\theta\text{-Al}_2\text{O}_3$). This dynamic behav-

ior of the transitional aluminas with the generation of coordinative unsaturation on the Al cation is in large part responsible for some of their more important properties such as acidity.

The discussion presented here emphasizes that the microcrystalline nature of γ - Al_2O_3 provides a rationale for the limitation of surface area to ~ 200 m^2/gm . This model therefore suggests that transitional aluminas with reported values of higher surface areas most probably contain a considerable amorphous component. The fact that large single crystals of γ - Al_2O_3 have never been grown is not a reflection of experimental technique but rather of the physical constraints of the particle size. Differences in γ - and η - Al_2O_3 arise from morphological differences relating to the relative amounts of different surface planes exposed. Variations in synthesis conditions create these differences. Changes in pore structure and volume can be achieved within certain definite limits (0.04–1.3 cm^3/g) by varying the stacking configuration of the γ - Al_2O_3 particles. Only when the requirements for crystallinity and interparticle contact are relaxed, as for example in Aerogels, do larger surface areas and pore volumes occur (19, 20).

ACKNOWLEDGMENT

The author thanks the following people for helpful discussions about the model presented here: John Longo, Larry Murrell, Gary McVicker, Wim Pieters, and Larry Sherman.

REFERENCES

1. Ratnasamy, P., and Sivasanker, S., *Catal. Rev.-Sci. Eng.* **22(3)**, 401 (1980).

2. Furimsky, E., *Catal. Rev.-Sci. Eng.* **22(3)**, 371 (1980).
3. Ciapetta, F. G., and Wallace, D. N., *Catal. Rev.* **5**, 67 (1971).
4. Lippens, B. C., thesis, Delft (Holland), 1961.
5. Peri, J. B., *J. Phys. Chem.* **69**, 220 (1965).
6. Dabrowski, J. E., Butt, J. B., and Harding, B., *J. Catal.* **18(3)**, 297 (1970).
7. Knozinger, H., and Ratnasamy, P., *Catal. Rev.-Sci. Eng.* **17(1)**, 31 (1978).
8. Klug, H. P., and Alexander, L. E., "X-Ray Diffraction Procedures," Wiley, New York, 1974.
9. Basila, M. R., *Appl. Spectrosc. Rev.* **1(2)**, 289 (1968).
10. Hair, M. L., "Infrared Spectroscopy in Surface Chemistry," Chap. V. Dekker, New York, 1967.
11. Verwey, J. W., and Heilmann, E. L., *J. Chem. Phys.* **15**, 174 (1947).
12. Blasse, G., *Philips Res. Rep. Suppl.* **3**, 1 (1964).
13. Dunitz, J. D., and Orgel, L. E., *J. Phys. Chem. Solids* **3**, 318 (1957).
14. Wells, A. F., "Structural Inorganic Chemistry," Oxford Press, London, 1962.
15. de Boer, J. H., and Houben, G. M. M., in "Proceedings 2nd International Symposium Reactive Solids, Gothenburg," 1952.
16. Satterfield, C. N., "Heterogeneous Catalysis in Practice," McGraw-Hill, New York, 1980.
17. Wilson, S. J., *J. Solid. State Chem.* **30**, 247 (1979).
18. Shannon, R. D., and Prewitt, C. T., *Acta Crystallogr.* **B25**, 928 (1969).
19. Teichner, S. J., Nicolaon, G. A., Vicarini, M. A., and Gardes, G. E. E., *Adv. Colloid Interface Sci.* **5**, 245 (1976).
20. Ghorbel, H., Hoang-Van, C., and Teichner, S. J., *J. Catal.* **30**, 298 (1973).

S. SOLED

Corporate Research-Science Laboratories
Exxon Research and Engineering Company
Linden, New Jersey 07036

Received October 21, 1982